Technical Reports (CIS)

Department of Computer & Information Science

January 1996

Bernstein Polynomials for Radiative Transfer Computations

Min-Zhi Shao
University of Pennsylvania

Norman I. Badler
University of Pennsylvania, badler@seas.upenn.edu

University of Pennsylvania Department of Computer and Information Science Technical Report No. MS-CIS-96-01.

Bernstein Polynomials for Radiative Transfer Computations

Abstract

In this paper we propose using planar and spherical Bernstein polynomials over triangular domain for radiative transfer computations. In the planar domain, we propose using piecewise Bernstein basis functions and symmetric Gaussian quadrature formulas over triangular elements for high quality radiosity solution. In the spherical domain, we propose using piecewise Bernstein basis functions over a geodesic triangulation to represent the radiance function. The representation is intrinsic to the unit sphere, and may be efficiently stored, evaluated, and subdivided by the de Casteljau algorithm. The computation of other fundamental radiometric quantities such as vector irradiance and reflected radiance may be reduced to the integration of the piecewise Bernstein basis functions on the unit sphere. The key result of our work is a simple geometric integration algorithm based on adaptive domain subdivision for the Bernstein-Bézier polynomials over a geodesic triangle on the unit sphere.

Comments

University of Pennsylvania Department of Computer and Information Science Technical Report No. MS-CIS-96-01.

Bernstein Polynomials
for Radiative Transfer Computations

MS-CIS-96-01

Min-Zhi Shao
Norman I. Badler

University of Pennsylvania
School of Engineering and Applied Science
Computer and Information Science Department
Philadelphia, PA 19104-6389

1996

Bernstein Polynomials for Radiative Transfer Computations

Min-Zhi Shao and Norman I. Badler

Department of Computer and Information Science
University of Pennsylvania

January 1996
Technical Report MS-CIS-96-01

Abstract

In this paper we propose using planar and spherical Bernstein polynomials over triangular domain for radiative transfer computations. In the planar domain, we propose using piecewise Bernstein basis functions and symmetric Gaussian quadrature formulas over triangular elements for high quality radiosity solution. In the spherical domain, we propose using piecewise Bernstein basis functions over a geodesic triangulation to represent the radiance function. The representation is intrinsic to the unit sphere, and may be efficiently stored, evaluated, and subdivided by the de Casteljau algorithm. The computation of other fundamental radiometric quantities such as vector irradiance and reflected radiance may be reduced to the integration of the piecewise Bernstein basis functions on the unit sphere. The key result of our work is a simple geometric integration algorithm based on adaptive domain subdivision for the Bernstein-Bézier polynomials over a geodesic triangle on the unit sphere.

CR Categories and Subject Descriptors: I.3.5 [Computational Geometry and Object Modeling]: Geometric Algorithms; I.3.7 [Computer Graphics]: Three-Dimensional Graphics and Realism.

Additional Key Words and Phrases: barycentric coordinates, barycentric subdivision, Bernstein polynomials, de Casteljau algorithm, Gaussian quadrature, radiance, radiosity method, spherical integration, spherical triangle, vector irradiance.

1 Introduction

The representation of radiance and reflectance functions on the unit sphere is essential in radiative transfer problems [23]. Available techniques include spherical harmonics, geodesic subdivision, spherical wavelets, and spherical monomials.

The spherical harmonics [21] are the products of associated Legendre functions with periodic trigonometric functions. Since they form an orthonormal basis in the Hilbert space over the unit sphere, it is often convenient to use them to describe and manipulate direction-dependent functions. In computer graphics, spherical harmonics have been used to represent bidirectional reflectance distribution functions (BRDFs) [8, 30], incident radiance functions [8], reflected radiance functions [26], and scattering radiance functions in volume densities [18].

Because the basis functions are globally supported over the entire unit sphere, the spherical harmonic representation is often prone to the Gibbs phenomenon [27, p. 272], especially for discontinuous and highly directional functions. In addition, since BRDFs and reflected radiance functions are usually defined on the hemisphere, the overshoot and oscillations may be worsened along the equator, although the symmetry in the basis functions can be cleverly exploited to a certain extent [30]. When spherical harmonics are used to describe incident radiance functions, the situation may be even worse. By analogy with the radiosity method, it is like using a single element for the whole environment. Except for simple and special cases, we know that the results will be largely undesirable. It is also noted that the spherical harmonic representation is not intrinsic; in other words, it is coordinate-dependent.

A different approach is to use discrete data structures rather than smooth basis functions. Recently, a hierarchical geodesic sphere construction with adaptive subdivision has been proposed to approximate the BRDFs in terms of reflected and incident flux density ratios [15]. This representation tends to be more compact and accurate but lacks analytical expressions. New techniques, such as spherical wavelet algorithms [20, 25], may be used to further compress the data.

A direct motivation of this paper is Arvo's recent work on irradiance tensors [5]. Due to the generalized Stokes's theorem, the key result of the irradiance tensor paper is a recurrence relation for spherical monomials $x^i y^j z^k$ integrated over any measurable region on the sphere. For certain geometries such as polygons, it is shown that the resulting boundary integrals can be expressed in closed form. This implies that for BRDFs and incident radiance functions that are polynomials over the sphere, the reflected radiance functions can be evaluated analytically in polyhedral environments. In particular, when the integrated functions are defined as the moments about an axis (which form a special class of spherical polynomials), direct lighting effects such as illumination from directional area sources and view-dependent Phong-like glossy reflection can be simulated analytically.

In general, however, it is not numerically efficient and stable to represent an arbitrary spherical function such as an incident radiance function in terms of spherical polynomials, for two identified reasons. First, like spherical harmonics, the spherical polynomials are globally supported over the sphere and the representation is coordinate-dependent. Second, there is an approximate linear dependence between the members of the spherical monomial family $\{x^i y^j z^k\}$. If we use the least squares approximation, this approximate linear dependence implies that the resulting matrix equation will be ill-conditioned and the round-off errors may be amplified significantly. For the simplest monomials x^i defined in a line segment, it is known that it is virtually hopeless to solve the least squares matrix equation for the closest polynomial of degree ten [28, p. 178]. For the same reason, there may also be difficulties in using the approximating polynomial representation for computing values of the original function [10, p. 119].

From a different point of view, if we want to approximate a function at a point and its immediate neighborhood, by the Taylor expansion $f(x) = \sum_{i=0}^{\infty} x^i f^{(i)}(0)/i!$, the set of monomials x^i should be a natural choice for basis functions (power basis). However, if we want to approximate a function over an interval or a region, instead of using derivatives, we need integrals. For efficient approximation, this requires orthogonality or good linear independence for basis functions. One choice is to use globally supported orthogonal bases such as harmonic functions and Legendre polynomials. Another choice is to sacrifice the orthogonality for basis functions with local support, good regularity, and strong linear independence. A popular choice in this camp is the piecewise polynomials. This is the choice that we are going to investigate in this paper.

We propose using the piecewise spherical Bernstein basis functions over a geodesic triangulation to represent the radiance function. The representation is intrinsic to the unit sphere, and may be efficiently stored, evaluated, and subdivided by the numerically stable de Casteljau algorithm. The computation of other fundamental radiometric quantities such as vector irradiance and reflected radiance may be reduced to the integration of the piecewise Bernstein basis functions on the unit sphere. The key result of our work is a simple geometric integration algorithm based on adaptive domain subdivision for the Bernstein-Bézier polynomials over a geodesic triangle on the unit sphere.

2 Bernstein Polynomials

2.1 Planar Triangle

Let $\mathbf{a}$, $\mathbf{b}$, $\mathbf{c}$ be vertices of a nonsingular triangle in plane P in $\mathbf{R}^3$. For any point $\mathbf{p}$ inside the triangle, there always exist nonnegative real numbers u, v, w such that

$$\mathbf{p} = u\mathbf{a} + v\mathbf{b} + w\mathbf{c} \tag{1}$$

and

$$u + v + w = 1. \tag{2}$$

Since triangle $\triangle\mathbf{abc}$ is nonsingular, by solving the linear system (1) and (2) (note that point $\mathbf{p}$ is constrained in the plane of $\triangle\mathbf{abc}$), we have

$$u = \frac{\text{area}\,(\triangle\mathbf{pbc})}{\text{area}\,(\triangle\mathbf{abc})}, \qquad v = \frac{\text{area}\,(\triangle\mathbf{apc})}{\text{area}\,(\triangle\mathbf{abc})}, \qquad w = \frac{\text{area}\,(\triangle\mathbf{abp})}{\text{area}\,(\triangle\mathbf{abc})}, \tag{3}$$

where

$$\text{area}\,(\triangle\mathbf{abc}) = \frac{1}{2}\begin{vmatrix} a_x & b_x & c_x \\ a_y & b_y & c_y \\ 1 & 1 & 1 \end{vmatrix}. \tag{4}$$

The uniquely defined (u, v, w) are called the barycentric coordinates of point $\mathbf{p}$ with respect to $\mathbf{a}$, $\mathbf{b}$, $\mathbf{c}$ [12]; see Figure 1. With the geometric interpretation from the equations in (3), it is clear that barycentric coordinates are intrinsic, i.e., they only depend on the relative position of point $\mathbf{p}$ in $\triangle\mathbf{abc}$; in other words, they are coordinate-free or coordinate-independent.

In terms of barycentric coordinates, we may define the Bernstein polynomials of degree n over domain $\triangle\mathbf{abc}$

$$B^n_{i,j,k}(u, v, w) = \frac{n!}{i!j!k!}u^i v^j w^k, \qquad i + j + k = n \tag{5}$$

and $B^n_{i,j,k}(u, v, w) = 0$ if any of i, j, k is negative [12]. Note that they are bivariate functions because of the identity (2). By induction on the degree n, it can be shown that $B^n_{i,j,k}(u, v, w)$ are linearly independent. That is, they form a basis for all polynomials of total degree n that are defined over $\triangle\mathbf{abc}$. We list some basic analytical properties of the Bernstein polynomials; for details and other elegant geometric properties such as de Casteljau algorithm, degree elevation, subdivision formulas, and continuity conditions, see, e.g., [12, 11].

1. Recursion:

$$B^n_{i,j,k}(u, v, w) = uB^{n-1}_{i-1,j,k}(u, v, w) + vB^{n-1}_{i,j-1,k}(u, v, w) + wB^{n-1}_{i,j,k-1}(u, v, w), \qquad i + j + k = n. \tag{6}$$

2. Partition of unity:

$$\sum_{i+j+k=n} B^n_{i,j,k}(u, v, w) = 1. \tag{7}$$

3. Differentiation:

$$D^m_{(\bar{u},\bar{v},\bar{w})}B^n_{i,j,k}(u, v, w) = \frac{n!}{(n-m)!}\sum_{r+s+t=m} B^m_{r,s,t}(\bar{u}, \bar{v}, \bar{w})B^{n-m}_{i-r,j-s,k-t}(u, v, w), \qquad i+j+k = n, \tag{8}$$

   where $D^m_{(\bar{u},\bar{v},\bar{w})}$ is the mth order directional derivative along vector $(\bar{u}, \bar{v}, \bar{w}) = (u_2 - u_1, v_2 - v_1, w_2 - w_1)$ for two points (u_1, v_1, w_1) and (u_2, v_2, w_2) in domain $\triangle\mathbf{abc}$. Notice that $\bar{u} + \bar{v} + \bar{w} = 0$.

4. Integration:
$$\int_A B^n_{i,j,k}(u,v,w)\,dA = \frac{A}{\binom{n+2}{2}}, \qquad i+j+k=n, \tag{9}$$
where A is the area of domain $\triangle\mathbf{abc}$. Notice that $\binom{n+2}{2}$ is the dimension of Bernstein polynomials over the triangle. This means that the Bernstein polynomials partition the unity with equal integrals over the domain; in other words, they are equally weighted as basis functions.

Bernstein polynomials over triangular domain (Bézier triangle) are extremely important in surface design, data fitting and interpolation, and elsewhere. It has been shown that numerically they are inherently much more stable than the monomials [13, 14]. In high quality radiosity solution, they may be a natural choice for piecewise basis functions over triangular elements generated by discontinuity meshing [17, 19] or isolux meshing [4].

To evaluate the kernel projections in radiosity method, the Gaussian quadratures [10, p. 302] may be used. They have also been derived for simplexes [16]. The formulas can be made symmetric in barycentric coordinates, i.e., if a sample point (ξ,η,ζ) occurs, so do all its permutations. Figure 2 lists the first few quadrature rules over a triangle of area A,
$$\int_A f\,dA = A\sum_{i=1}^{n} w_i f(\xi_i,\eta_i,\zeta_i), \tag{10}$$
where (ξ_i,η_i,ζ_i) are the barycentric coordinates of the ith sampling point and w_i is the weight associated with it. For higher order formulas, see [9].

2.2 Spherical Triangle

Let S^2 be the unit sphere in $\mathbf{R}^3$ with center at the origin, and $\mathbf{a}$, $\mathbf{b}$, $\mathbf{c}$ be a set of linearly independent unit vectors which form a nonsingular geodesic triangle $\hat{\triangle}\mathbf{abc}$ on S^2; see Figure 3. For any unit vector $\mathbf{p}$ that points inside the spherical triangle, there always exist nonnegative real numbers u, v, w such that
$$\mathbf{p} = u\mathbf{a} + v\mathbf{b} + w\mathbf{c}. \tag{11}$$

Since $\mathbf{a}$, $\mathbf{b}$, $\mathbf{c}$ are linearly independent, by solving the linear system (11), we have
$$u = \frac{\det(\mathbf{p},\mathbf{b},\mathbf{c})}{\det(\mathbf{a},\mathbf{b},\mathbf{c})}, \qquad v = \frac{\det(\mathbf{a},\mathbf{p},\mathbf{c})}{\det(\mathbf{a},\mathbf{b},\mathbf{c})}, \qquad w = \frac{\det(\mathbf{a},\mathbf{b},\mathbf{p})}{\det(\mathbf{a},\mathbf{b},\mathbf{c})}, \tag{12}$$
where
$$\det(\mathbf{a},\mathbf{b},\mathbf{c}) = \begin{vmatrix} a_x & b_x & c_x \\ a_y & b_y & c_y \\ a_z & b_z & c_z \end{vmatrix}. \tag{13}$$

The uniquely defined (u, v, w) are called the spherical barycentric coordinates of spherical point $\mathbf{p}$ with respect to $\mathbf{a}$, $\mathbf{b}$, $\mathbf{c}$. They were first introduced by Möbius in the last century and rediscovered recently by Alfeld et al. [2], from where we adopt the definitions.

The equations in (12) also give a geometric interpretation of the spherical barycentric coordinates, i.e.,

$$u = \frac{\text{volume}\,(O\{\mathbf{p},\mathbf{b},\mathbf{c}\})}{\text{volume}\,(O\{\mathbf{a},\mathbf{b},\mathbf{c}\})}, \quad v = \frac{\text{volume}\,(O\{\mathbf{a},\mathbf{p},\mathbf{c}\})}{\text{volume}\,(O\{\mathbf{a},\mathbf{b},\mathbf{c}\})}, \quad w = \frac{\text{volume}\,(O\{\mathbf{a},\mathbf{b},\mathbf{p}\})}{\text{volume}\,(O\{\mathbf{a},\mathbf{b},\mathbf{c}\})}, \tag{14}$$

where $O\{\mathbf{a},\mathbf{b},\mathbf{c}\}$ denotes the (planar) tetrahedron defined by the origin and spherical points $\mathbf{a}$, $\mathbf{b}$, $\mathbf{c}$. This implies that the definition is intrinsic, i.e., the spherical barycentric coordinates are invariant under rotation or are coordinate-free.

Notice that, in the planar case the barycentric coordinates interpolate points in a plane P in $\mathbf{R}^3$, but in the spherical case they interpolate points on the unit sphere S^2 in $\mathbf{R}^3$ or equivalently interpolate unit vectors in $\mathbf{R}^3$. Although the definitions look similar, S^2 is always special. First, from the equations in (12), it is easily seen that the spherical barycentric coordinates u, v, w are homogeneous linear functions of $\mathbf{p}$. Second, they are linearly independent (let $\mathbf{p}$ be $\mathbf{a}$, $\mathbf{b}$, $\mathbf{c}$ respectively in a linear combination of u, v, w). Third,

$$u + v + w > 1 \tag{15}$$

for any unit vector $\mathbf{p}$ that points inside the spherical triangle. This is immediate from the geometric interpretation (14). Consequently, the spherical barycentric coordinates are not barycentric coordinates in the conventional sense. They do not partition the unity. In fact, it has been proved that such coordinates (satisfying a basic set of conditions drawn from fundamental properties of barycentric coordinates in the plane) do not exist on the sphere [7]. Here we clearly see the imprint of S^2. Recall that, e.g., $\alpha + \beta + \gamma > \pi$, where α, β, γ are three internal angles of a spherical triangle (consider Girard's formula for the area of spherical triangle).

Similar to the planar case, in terms of spherical barycentric coordinates, we may define the spherical Bernstein polynomials of degree n over domain $\triangle\mathbf{abc}$

$$B^n_{i,j,k}(u, v, w) = \frac{n!}{i!j!k!} u^i v^j w^k, \qquad i + j + k = n \tag{16}$$

and $B^n_{i,j,k}(u, v, w) = 0$ if any of i, j, k is negative. It is shown in [2, 3] that they are homogeneous trivariate basis functions and possess virtually all of the properties of the classical planar Bernstein polynomials, despite the results in [7]. However, formulas (7) and (9) are no longer valid. The failure of partition of unity is because of the inequality (15). We shall discuss the integration over spherical triangle in the next section.

3 Radiative Transfer Computations

3.1 Radiance Representation

Radiance [23, p. 28], denoted by $L(\mathbf{x}, \mathbf{p})$, describes the flow of radiant flux into a unit projected area at point $\mathbf{x} \in \mathbf{R}^3$ through a unit solid angle in direction $\mathbf{p} \in S^2$ [$\mathrm{W} \cdot \mathrm{m}^{-2} \cdot \mathrm{sr}^{-1}$]. It is considered the most important radiometric concept since all other radiometric quantities can be naturally defined and calculated in terms of it. The totality of all values $L(\mathbf{x}, \mathbf{p})$ as $\mathbf{p}$ ranges over the unit sphere is called the radiance distribution function [23, p. 29] at point $\mathbf{x}$, denoted by $L(\mathbf{x}, \cdot)$.

We propose to represent $L(\mathbf{x}, \cdot)$ in terms of piecewise Bernstein polynomials over a spherical triangulation (a set of geodesic triangles in which any two of them intersect only at a common vertex or along an edge). Like their planar counterparts, the spherical Bernstein polynomials can be efficiently stored, evaluated, differentiated, subdivided, and joined together. We shall not go into details of various aspects of the representation techniques, e.g., interpolation or approximation. For a sophisticated discussion, see [3].

Without loss of generality, we may assume that $\mathbf{x}$ is located at the origin (and thus drop it from $L(\mathbf{x}, \mathbf{p})$) and consider the radiance distribution function over a single spherical triangle $\triangle\mathbf{abc}$,

$$L(\mathbf{p}) = \sum_{i+j+k=n} c_{i,j,k} B^n_{i,j,k}(u, v, w), \tag{17}$$

where unit vector $\mathbf{p}$ points inside the triangle, and $c_{i,j,k}$ are real coefficients of the Bernstein basis functions. It is also called a spherical Bernstein-Bézier polynomial of degree n [2]. Geometrically, the function $L(\mathbf{p})$ may be viewed as a surface over domain $\triangle\mathbf{abc}$ whose radial height is its value.

To evaluate the radiance distribution function at a direction $\mathbf{p}$ with spherical barycentric coordinates (u, v, w), we may use the classical de Casteljau algorithm [2].

de Casteljau Algorithm.

for $i + j + k = n$:
  $c^0_{i,j,k} = c_{i,j,k}$;
for $r = 1, 2, \ldots, n$:
  for $i + j + k = n - r$:
    $c^r_{i,j,k} = u * c^{r-1}_{i+1,j,k} + v * c^{r-1}_{i,j+1,k} + w * c^{r-1}_{i,j,k+1}$;
$L(\mathbf{p}) = c^n_{0,0,0}$;
end

The algorithm is surprisingly simple. Numerically, it is also very efficient and stable due to the geometric nature of barycentric interpolation. The round-off error bound grows only linearly with degree n, even though the number of arithmetic operations grows quadratically [13].

Once again, we emphasize that the radiance representation is intrinsic to S^2.

3.2 Vector Irradiance

Irradiance [23, p. 24], denoted by $H(\mathbf{x}, \mathbf{n})$, describes the flow of radiant flux into a unit area at point x on a real surface with normal $\mathbf{n}$ [$\mathrm{W} \cdot \mathrm{m}^{-2}$]. Net irradiance [23, p. 38], denoted by $\bar{H}(\mathbf{x}, \mathbf{n})$, describes the flow of radiant flux into a unit area at point x on a hypothetical surface with normal $\mathbf{n}$ [$\mathrm{W} \cdot \mathrm{m}^{-2}$]. By definition, we have

$$H(\mathbf{x}, \mathbf{n}) = \int_{S^2_+(\mathbf{n})} L(\mathbf{x}, \mathbf{p})\, \mathbf{n} \cdot \mathbf{p}\, d\Omega(\mathbf{p}) \tag{18}$$

and

$$\bar{H}(\mathbf{x}, \mathbf{n}) = \int_{S^2} L(\mathbf{x}, \mathbf{p})\, \mathbf{n} \cdot \mathbf{p}\, d\Omega(\mathbf{p}), \tag{19}$$

where $S^2_+(\mathbf{n})$ denotes the unit hemisphere defined by $\mathbf{n}$, and $\Omega(\mathbf{p})$ denotes the solid angle measure in direction $\mathbf{p}$.

In terms of radiance, we may define another useful irradiance function, vector irradiance [23, p. 39], as

$$\mathbf{H}(\mathbf{x}) = \int_{S^2} L(\mathbf{x}, \mathbf{p})\, \mathbf{p}\, d\Omega(\mathbf{p}). \tag{20}$$

In contrast with radiance, vector irradiance gives a measure of the predominant direction of radiant flux at point x without emphasizing the magnitude of various component flows. From Equations (19) and (20), we have

$$\bar{H}(\mathbf{x}, \mathbf{n}) = \mathbf{n} \cdot \mathbf{H}(\mathbf{x}). \tag{21}$$

The same equation holds for irradiance $H(\mathbf{x}, \mathbf{n})$ if vector irradiance is integrated over the hemisphere above a real surface at point x. For this reason, the vector integration (20) is fundamental in many radiative transfer problems.

When the radiance distribution function is represented by Equation (17), with the same assumptions, we have vector irradiance at the origin

$$\begin{aligned} \mathbf{H} &= \int_A L(\mathbf{p})\, \mathbf{p}\, dA = \int_A \sum_{i+j+k=n} c_{i,j,k} B^n_{i,j,k}(u, v, w)\, (u\mathbf{a} + v\mathbf{b} + w\mathbf{c})\, dA \\ &= \sum_{i+j+k=n} c_{i,j,k} \int_A (uB^n_{i,j,k}(u, v, w)\, \mathbf{a} + vB^n_{i,j,k}(u, v, w)\, \mathbf{b} + wB^n_{i,j,k}(u, v, w)\, \mathbf{c})\, dA, \end{aligned} \tag{22}$$

where A is the area of domain $\triangle\mathbf{abc}$. Since $\mathbf{a}, \mathbf{b}, \mathbf{c}$ are constant unit vectors and

$$uB^n_{i,j,k}(u, v, w) = \frac{i+1}{n+1} B^{n+1}_{i+1,j,k}(u, v, w),$$

$$vB^n_{i,j,k}(u,v,w) = \frac{j+1}{n+1} B^{n+1}_{i,j+1,k}(u,v,w), \tag{23}$$
$$wB^n_{i,j,k}(u,v,w) = \frac{k+1}{n+1} B^{n+1}_{i,j,k+1}(u,v,w),$$

the evaluation of vector irradiance $\mathbf{H}$ may be reduced to the integration of Bernstein basis functions over a spherical triangle.

Unfortunately, as noted in [3], evaluating spherical polynomials is considerably more difficult than in the planar case and a simple explicit formula like (9) does not seem to exist. In general, the integrals of spherical Bernstein polynomials depend on not only the shape of the spherical triangle but the individual basis functions as well. Recurrence relations, however, may probably exist. We have found them for the circular Bernstein polynomials [1]; though in two dimensions, the formulas are already quite complicated. We decide to give up the effort after observing the following:

$$\sum_{i+j+k=n} \int_A B^n_{i,j,k}(u,v,w)\, dA = \int_A (u+v+w)^n\, dA. \tag{24}$$

Because of the inequality (15), the integrals of the basis functions diverge as n increases. Also note that u, v, w are not bounded (they approach infinity as planar triangle $\triangle\mathbf{abc}$ gets close to the origin). Numerically, these are not encouraging signs for an effective integration scheme.

In [3], a brute-force method has been suggested, i.e., first projecting the spherical polynomials from $\mathbf{\hat{\triangle}abc}$ onto $\triangle\mathbf{abc}$ and then using standard numerical integration techniques for the planar triangle.

In the next subsection, we shall seek a geometric integration approach that is coherent with the spherical barycentric coordinate system.

3.3 Spherical Integration

In the previous subsection, we have noticed that the integrals of spherical Bernstein basis functions diverge as degree n increases. By the nature of the radiance distribution function and Bernstein polynomials, however, integrals such as

$$\int_A L(\mathbf{p})\, dA = \int_A \sum_{i+j+k=n} c_{i,j,k} B^n_{i,j,k}(u,v,w)\, dA \tag{25}$$

should converge as n goes to infinity. The value of above integral is called the scalar irradiance (denoted by $h(\mathrm{x})$ [$\mathrm{W \cdot m^{-2}}$]) [23, p. 39]. Divided by the speed of light, it describes the radiant energy per unit volume at point x, called the radiant energy density (denoted by $u(\mathrm{x})$ [$\mathrm{J \cdot m^{-3}}$]) [23, p. 39].

The same argument goes to vector irradiance and other physically meaningful integrals. This leads us to investigate an integration algorithm that directly applies to the spherical

Bernstein-Bézier polynomials rather than individual Bernstein basis functions. That is, we consider using the coefficients $c_{i,j,k}$ to control and stabilize the integration.

We begin with barycentric domain subdivision [6, I, p. 82]. The barycentric subdivision of a planar triangle $\triangle\mathbf{abc}$ is a set of six triangles having one vertex at the center $(\mathbf{a}+\mathbf{b}+\mathbf{c})/3$ and opposite sides equal to each line segment in the barycentric subdivisions of edges $\mathbf{ab}$, $\mathbf{bc}$, $\mathbf{ca}$. We may iterate the process and generate a hexatree of triangles; for the first three levels, see Figure 4. Intuitively, the maximum diameter of all triangles approaches zero as the level of hexatree increases.

Similarly, we may define barycentric subdivision of a spherical triangle. For a nonsingular spherical triangle $\hat{\triangle}\mathbf{abc}$, we may use

$$\frac{\mathbf{a}+\mathbf{b}+\mathbf{c}}{\|\mathbf{a}+\mathbf{b}+\mathbf{c}\|} \tag{26}$$

for the center vertex and

$$\frac{\mathbf{a}+\mathbf{b}}{\|\mathbf{a}+\mathbf{b}\|}, \quad \frac{\mathbf{b}+\mathbf{c}}{\|\mathbf{b}+\mathbf{c}\|}, \quad \frac{\mathbf{c}+\mathbf{a}}{\|\mathbf{c}+\mathbf{a}\|} \tag{27}$$

for three additional middle vertices at the edges. Here $\|\cdot\|$ denotes the Euclidean norm in $\mathbf{R}^3$. Figure 5 shows a second level barycentric subdivision of a spherical triangle.

Next, we decompose the spherical Bernstein-Bézier polynomial in accordance with the subdivided domains. It turns out to be surprisingly simple due to the classical subdivision theorem [2].

Subdivision Theorem. Suppose $\sum_{i+j+k=n} c_{i,j,k}B^n_{i,j,k}(u,v,w)$ is a spherical Bernstein-Bézier polynomial over domain $\hat{\triangle}\mathbf{abc}$, and $c^r_{i,j,k}(r=0,1,\ldots,n)$ are the intermediate de Casteljau coefficients with respect to a point $\mathbf{v}$ lying in the spherical triangle. Then, for any spherical point $\mathbf{p} = u\mathbf{a}+v\mathbf{b}+w\mathbf{c} \in \hat{\triangle}\mathbf{abc}$, we have

$$\sum_{i+j+k=n} c_{i,j,k}B^n_{i,j,k}(u,v,w) = \begin{cases} \sum_{i+j+k=n} c^i_{0,j,k}B^n_{i,j,k}(u',v',w'), & \mathbf{p} = u'\mathbf{v}+v'\mathbf{b}+w'\mathbf{c} \in \hat{\triangle}\mathbf{vbc}, \\ \sum_{i+j+k=n} c^j_{i,0,k}B^n_{i,j,k}(u',v',w'), & \mathbf{p} = u'\mathbf{a}+v'\mathbf{v}+w'\mathbf{c} \in \hat{\triangle}\mathbf{avc}, \\ \sum_{i+j+k=n} c^k_{i,j,0}B^n_{i,j,k}(u',v',w'), & \mathbf{p} = u'\mathbf{a}+v'\mathbf{b}+w'\mathbf{v} \in \hat{\triangle}\mathbf{abv}. \end{cases} \tag{28}$$

The implication of above theorem to barycentric subdivision is obvious. We may proceed with the basis function decomposition in two steps, first using the center vertex and then the three additional edge vertices. It is noted that the three decompositions in the second step with respect to edge vertices are degenerate cases of the subdivision theorem. One circular Bernstein-Bézier polynomial [1] is generated in each decomposition. They may be simply discarded.

Based on the hierarchical barycentric subdivision, we may iterate the decomposition process and generate a hexatree of spherical Bernstein-Bézier polynomials. Intuitively, as the level of hexatree increases, $\triangle\mathbf{a}_l\mathbf{b}_l\mathbf{c}_l$ tends to $\hat{\triangle}\mathbf{a}_l\mathbf{b}_l\mathbf{c}_l$ (where l indexes the leaf triangles) with the maximum diameter of all triangles approaching zero. At the same time, the barycentric coordinates $(u_l(\mathbf{p}), v_l(\mathbf{p}), w_l(\mathbf{p}))$ with respect to $\hat{\triangle}\mathbf{a}_l\mathbf{b}_l\mathbf{c}_l$ approach $(u'_l(\mathbf{p}'), v'_l(\mathbf{p}'), w'_l(\mathbf{p}'))$ with respect to $\triangle \mathbf{a}_l\mathbf{b}_l\mathbf{c}_l$, where $\mathbf{p}' \in \triangle \mathbf{a}_l\mathbf{b}_l\mathbf{c}_l$ is the radial projection of spherical point $\mathbf{p} \in \hat{\triangle} \mathbf{a}_l\mathbf{b}_l\mathbf{c}_l$; see Figure 3. The proof is straightforward with the help of geometric interpretations (3) and (14).

It follows that for a sufficiently small spherical triangle $\hat{\triangle}\mathbf{a}_l\mathbf{b}_l\mathbf{c}_l$, we may approximate the spherical Bernstein-Bézier polynomial by its planar counterpart; from Equation (9),

$$\int_{A_l} \sum_{i+j+k=n} c_{i,j,k} B^n_{i,j,k}(u,v,w)\, dA_l \doteq \frac{A_l}{\binom{n+2}{2}} \sum_{i+j+k=n} c_{i,j,k}, \tag{29}$$

where A_l is the area of $\hat{\triangle}\mathbf{a}_l\mathbf{b}_l\mathbf{c}_l$. After a few steps of preliminary integral manipulations, it may be shown that the relative error ϵ^l_{r} of above approximation is in the order of

$$n(\frac{u_l - u'_l}{u_l} + \frac{v_l - v'_l}{v_l} + \frac{w_l - w'_l}{w_l}), \tag{30}$$

which retains its maximum value along vector $\mathbf{a}_l + \mathbf{b}_l + \mathbf{c}_l$ (again, think about the geometric interpretations (3) and (14)). This immediately leads to a global relative error measure ϵ_{r} which may be used as the terminating condition:

$$\max_l n(1 - \frac{\|\mathbf{a}_l + \mathbf{b}_l + \mathbf{c}_l\|}{3}), \tag{31}$$

or equivalently,

$$\max_l n(\Theta^2_{\mathbf{a}_l} + \Theta^2_{\mathbf{b}_l} + \Theta^2_{\mathbf{c}_l}), \tag{32}$$

where $\Theta_{\mathbf{a}_l}$, $\Theta_{\mathbf{b}_l}$, $\Theta_{\mathbf{c}_l}$ are angles between vector $\mathbf{a}_l + \mathbf{b}_l + \mathbf{c}_l$ and vectors $\mathbf{a}_l$, $\mathbf{b}_l$, $\mathbf{c}_l$, respectively. The relative error ϵ_{r} does not depend on $c_{i,j,k}$ while the absolute error ϵ_{a} clearly does. Also note that the degree of basis functions and the area of domain triangle are reciprocal for a constant relative error measure. This is consistent with the observation (24).

The area of a spherical triangle may be obtained by Girard's formula [6, II, p. 278]

$$\alpha + \beta + \gamma - \pi \tag{33}$$

and the fundamental formulas of spherical trigonometry (spherical cosine laws) [6, II, p. 286]

$$\begin{aligned} \cos a &= \cos b \cos c + \sin b \sin c \cos \alpha, \\ \cos b &= \cos c \cos a + \sin c \sin a \cos \beta, \\ \cos c &= \cos a \cos b + \sin a \sin b \cos \gamma, \end{aligned} \tag{34}$$

where α, β, γ and a, b, c are displayed in Figure 3.

The following is the pseudo-code of the integration algorithm.

Integration Algorithm.

$Integral(BBP(\hat{\triangle}\mathbf{abc}))$

if $\mathit{Termination}(\mathbf{a}, \mathbf{b}, \mathbf{c})$ **then**

  return $(\sum_{i+j+k=n} c_{i,j,k}) * \mathit{Area}(\triangle\mathbf{abc})/\binom{n+2}{2}$;

else

  $\mathit{Subdivision}(\triangle\mathbf{abc})$;

  return $\sum_{i=1}^{6} \mathit{Integral}(\mathit{BBP}(\triangle\mathbf{a}_i\mathbf{b}_i\mathbf{c}_i))$;

end

It should be noted that the corner angles are repeatedly subdivided in each level of the barycentric subdivision; see Figure 5. This may not be desirable in practice. For its conceptual simplicity, we choose to use barycentric subdivision to illustrate the integration algorithm. A simple binary subdivision scheme in accordance with the largest angle, though asymmetrical, may be a better choice for practical usage; see Figure 6.

Also note that the domain subdivision implies a simple visibility determination algorithm [29].

Because the approximating planar triangles are inscribed about the unit sphere, the integral computed in above algorithm increases monotonically. Richardson extrapolation [10, p. 269] may be used to accelerate the convergence.

3.4 Reflectance Function

Consider a surface point located at the origin with normal $\mathbf{n}$. Let $L(\mathbf{p})$ in Equation (17) be the radiance distribution function over a spherical triangle $\triangle\mathbf{abc}$. Then the reflected radiance at the surface point in the direction $\mathbf{q}$ may be expressed as

$$\begin{aligned} L(\mathbf{q}) &= \int_A \rho(\mathbf{p} \to \mathbf{q})\, L(\mathbf{p})\, \mathbf{n} \cdot \mathbf{p}\, dA \\ &= \int_A \rho(\mathbf{p} \to \mathbf{q}) \sum_{i+j+k=n} c_{i,j,k} B^n_{i,j,k}(u, v, w)\, (\mathbf{n} \cdot \mathbf{a}u + \mathbf{n} \cdot \mathbf{b}v + \mathbf{n} \cdot \mathbf{c}w)\, dA, \end{aligned} \tag{35}$$

where ρ denotes the bidirectional reflectance distribution function. Clearly, if $\rho(\mathbf{p} \to \mathbf{q})$ is represented as a polynomial of u, v, w then the reflected radiance $L(\mathbf{q})$ may be evaluated by the integration algorithm developed in the previous section.

For instance, when the reflectance admits the Phong distribution [22], i.e.,

$$\begin{aligned} \rho(\mathbf{p} \to \mathbf{q}) &= (\mathbf{v} \cdot \mathbf{p})^n = (\mathbf{v} \cdot \mathbf{a}u + \mathbf{v} \cdot \mathbf{b}v + \mathbf{v} \cdot \mathbf{c}w)^n \\ &= \sum_{i+j+k=n} (\mathbf{v} \cdot \mathbf{a})^i (\mathbf{v} \cdot \mathbf{b})^j (\mathbf{v} \cdot \mathbf{c})^k\, B^n_{i,j,k}(u, v, w), \end{aligned} \tag{36}$$

where $\mathbf{v} = (2\mathbf{n}\mathbf{n}^{\mathrm{T}} - \mathbf{I})\mathbf{q}$ is the mirror reflection of vector $\mathbf{q}$ with respect to surface normal $\mathbf{n}$, we see that it is a Bernstein-Bézier polynomial. For energy conservation, the above distribution should be normalized by constant $2\pi/(n+2)$ [5].

4 Conclusions

We have proposed using planar and spherical Bernstein polynomials over triangular domain for radiative transfer computations. In the planar case, we have proposed using piecewise Bernstein basis functions and symmetric Gaussian quadrature formulas over triangular elements for high quality radiosity solution. In the spherical case, we have proposed using piecewise Bernstein basis functions to obtain an intrinsic radiance distribution representation. Under the representation, the computation of vector irradiance and reflected radiance may be reduced to the integration of the Bernstein-Bézier polynomials over a geodesic triangle on the unit sphere. We have presented a simple and efficient algorithm by adaptive domain subdivision for this spherical integration. Due to the geometric nature of the de Casteljau algorithm, the evaluation and integration of the radiance function are numerically stable.

The generalization of barycentric coordinates and basic theory of the Bernstein polynomials to higher dimension is immediate [11]. It may be a natural topic to investigate the applications to radiosity method in the presence of a participating medium [24].

Another interesting problem for future research is the design of spherical wavelet algorithms for the Bernstein polynomials. The task may be benefited from the integration algorithm presented in this paper.

References

[1] P. Alfeld, M. Neamtu, and L. L. Schumaker, "Circular Bernstein-Bézier polynomials," in *Mathematical Methods for Curves and Surfaces*, M. Dæhlen, T. Lyche, and L. L. Schumaker, Eds., 11–20, Vanderbilt University Press, Nashville, Tennessee, 1995.

[2] P. Alfeld, M. Neamtu, and L. L. Schumaker, "Bernstein-Bézier polynomials on spheres and sphere-like surfaces," *Computer Aided Geometric Design*, to appear.

[3] P. Alfeld, M. Neamtu, and L. L. Schumaker, "Fitting scattered data on sphere-like surfaces using spherical splines," *Journal of Computational and Applied Mathematics*, to appear.

[4] J. Arvo, "The irradiance Jacobian for partially occluded polyhedral sources," *Proc. ACM Siggraph*, 343–350, July 1994.

[5] J. Arvo, "Applications of irradiance tensors to the simulation of non-Lambertian phenomena," *Proc. ACM Siggraph*, 335–342, August 1995.

[6] M. Berger, *Geometry*, Springer-Verlag, Berlin, 1987.

[7] J. L. Brown and A. J. Worsey, “Problems with defining barycentric coordinates for the sphere,” *Mathematical Modelling and Numerical Analysis*, 26:37–49, 1992.

[8] B. Cabral, N. Max, and R. Springmeyer, “Bidirectional reflection functions from surface bump maps,” *Proc. ACM Siggraph*, 273–281, July 1987.

[9] G. R. Cowper, “Gaussian quadrature formulas for triangles,” *International Journal for Numerical Methods in Engineering*, 7:405-408, 1973.

[10] G. Dahlquist and A. Björck, *Numerical Methods*, Prentice-Hall, Englewood Cliffs, New Jersey, 1974.

[11] C. de Boor, “B-form basics,” in *Geometric Modeling: Algorithms and New Trends*, G. E. Farin, Ed., 131–148, Society for Industrial and Applied Mathematics, Philadelphia, 1987.

[12] G. Farin, “Triangular Bernstein-Bézier patches,” *Computer Aided Geometric Design*, 3:83–127, August 1986.

[13] R. Farouki and V. Rajan, “On the numerical condition of polynomials in Bernstein form,” *Computer Aided Geometric Design*, 4:191–216, November 1987.

[14] R. Farouki and V. Rajan, “Algorithms for polynomials in Bernstein form,” *Computer Aided Geometric Design*, 5:1–26, June 1988.

[15] J. S. Gondek, G. W. Meyer, and J. G. Newman, “Wavelength dependent reflectance functions,” *Proc. ACM Siggraph*, 213–220, July 1994.

[16] P. C. Hammer, O. J. Marlowe, and A. H. Stroud, “Numerical integration over simplexes and cones,” *Mathematical Tables and Other Aids to Computation*, 10:130-137, 1956.

[17] P. S. Heckbert, “Simulating global illumination using adaptive meshing,” Ph.D. thesis, Department of Electrical Engineering and Computer Sciences, University of California at Berkeley, June 1991.

[18] J. T. Kajiya and B. P. Von Herzen, “Ray tracing volume densities,” *Proc. ACM Siggraph*, 165–174, July 1984.

[19] D. Lischinski, F. Tampieri, and D. P. Greenberg, “Discontinuity meshing for accurate radiosity,” *IEEE Computer Graphics and Applications*, 12:25–39, November 1992.

[20] M. Lounsbery, T. D. DeRose, and J. Warren, “Multiresolution analysis for surfaces of arbitrary topological type,” Technical Report 93-10-05, Department of Computer Science and Engineering, University of Washington, October 1993.

[21] C. Müller, *Spherical Harmonics*, Springer-Verlag, Berlin, 1966.

[22] B. T. Phong, "Illumination for computer generated pictures," *Communications of the ACM*, 18:311–317, June 1975.

[23] R. W. Preisendorfer, *Radiative Transfer on Discrete Spaces*, Pergamon Press, Oxford, England, 1965.

[24] H. E. Rushmeier and K. E. Torrance, "The zonal method for calculating light intensities in the presence of a participating medium," *Proc. ACM Siggraph*, 293–302, July 1987.

[25] P. Schröder and W. Sweldens, "Spherical wavelets: Efficiently representing functions on the sphere," *Proc. ACM Siggraph*, 161–172, August 1995.

[26] F. X. Sillion, J. R. Arvo, S. H. Westin, and D. P. Greenberg, "A global illumination solution for general reflectance distributions," *Proc. ACM Siggraph*, 187–196, July 1991.

[27] G. Strang, *Introduction to Applied Mathematics*, Wellesley-Cambridge, Wellesley, Massachusetts, 1986.

[28] G. Strang, *Linear Algebra and Its Applications*, Harcourt Brace Jovanovich, San Diego, California, 1988.

[29] I. E. Sutherland, R. F. Sproull, and R. A. Schumacker, "A characterization of ten hidden-surface algorithms," *ACM Computing Surveys*, 6:1–55, March 1974.

[30] S. H. Westin, J. R. Arvo, and K. E. Torrance, "Predicting reflectance functions from complex surfaces," *Proc. ACM Siggraph*, 255–264, July 1992.

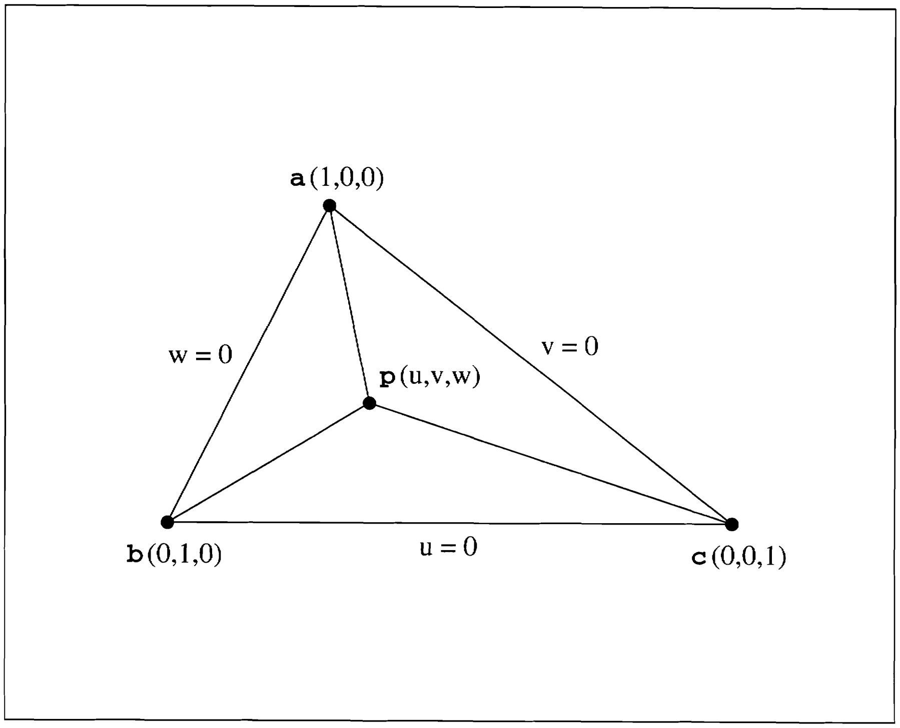

Figure 1: Planar barycentric coordinates.

figure	error	barycentric coordinates	weights
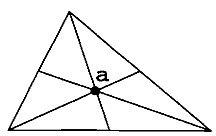	$O(h^2)$	**a** (1/3, 1/3, 1/3)	1
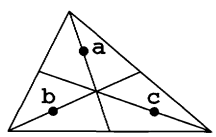	$O(h^3)$	**a** (2/3, 1/6, 1/6) **b** (1/6, 2/3, 1/6) **c** (1/6, 1/6, 2/3)	1/3 1/3 1/3
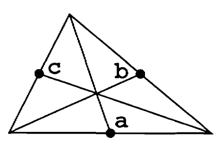	$O(h^3)$	**a** (0 , 1/2, 1/2) **b** (1/2, 0 , 1/2) **c** (1/2, 1/2, 0)	1/3 1/3 1/3
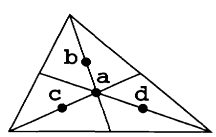	$O(h^4)$	**a** (1/3, 1/3, 1/3) **b** (3/5, 1/5, 1/5) **c** (1/5, 3/5, 1/5) **d** (1/5, 1/5, 3/5)	−27/48 25/48 25/48 25/48

Figure 2: Gaussian quadrature formulas for the triangle.

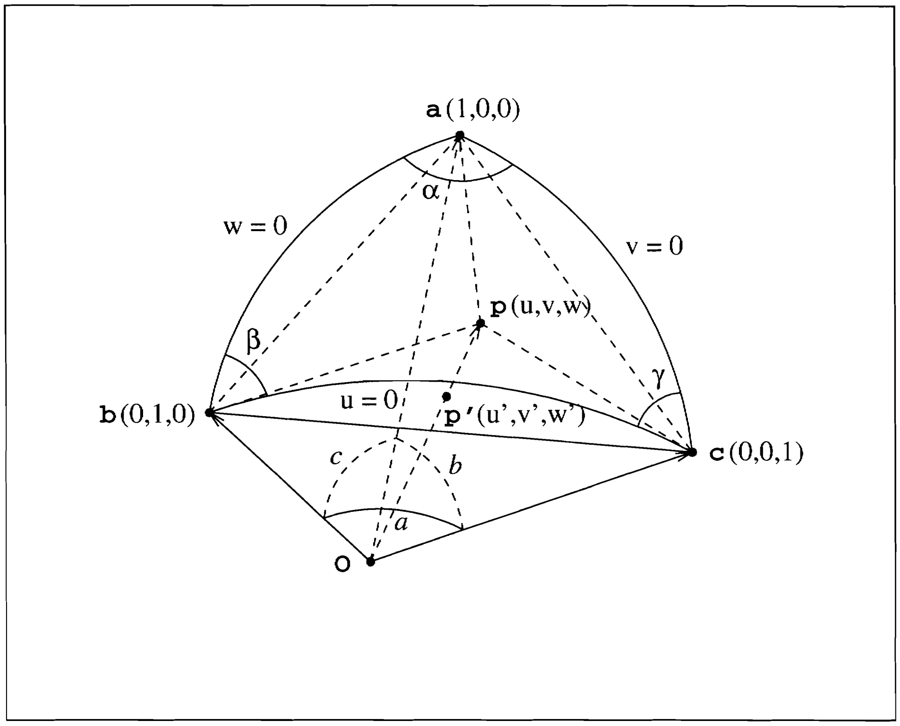

Figure 3: Spherical barycentric coordinates.

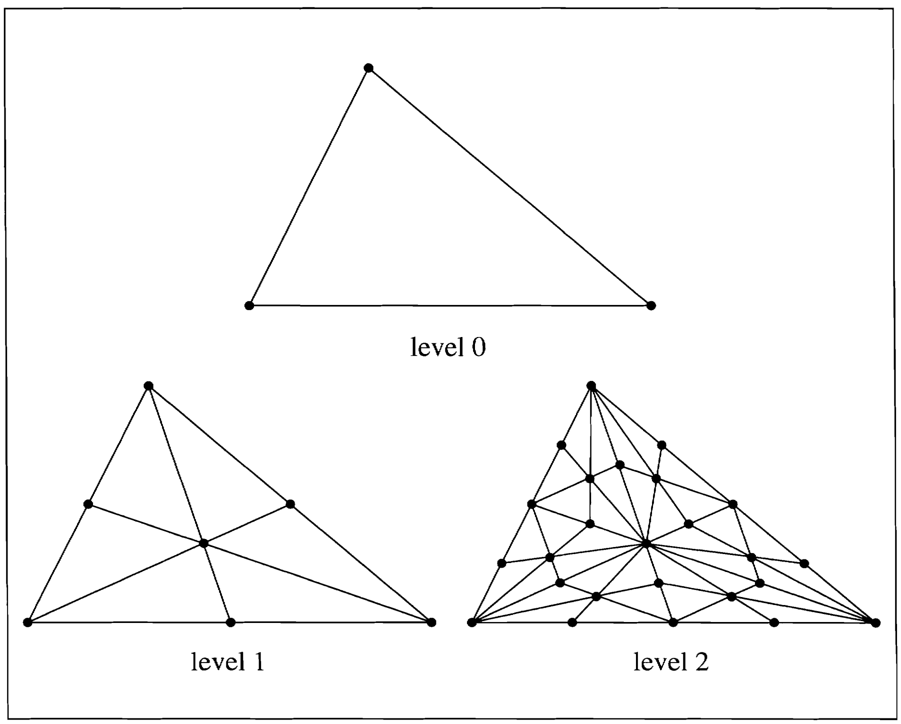

Figure 4: Planar barycentric subdivision.

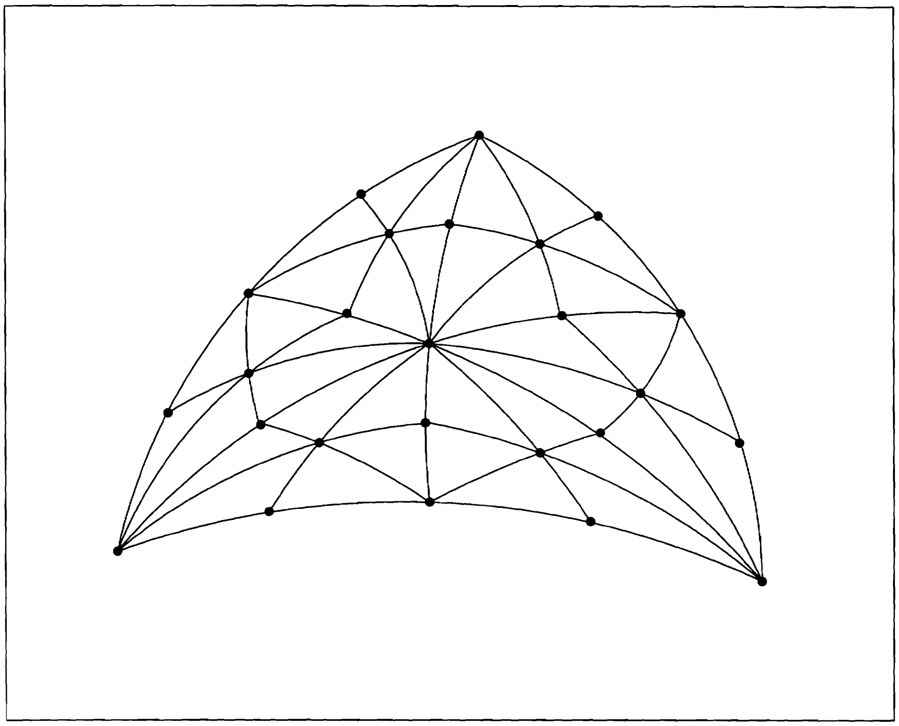

Figure 5: Spherical barycentric subdivision.

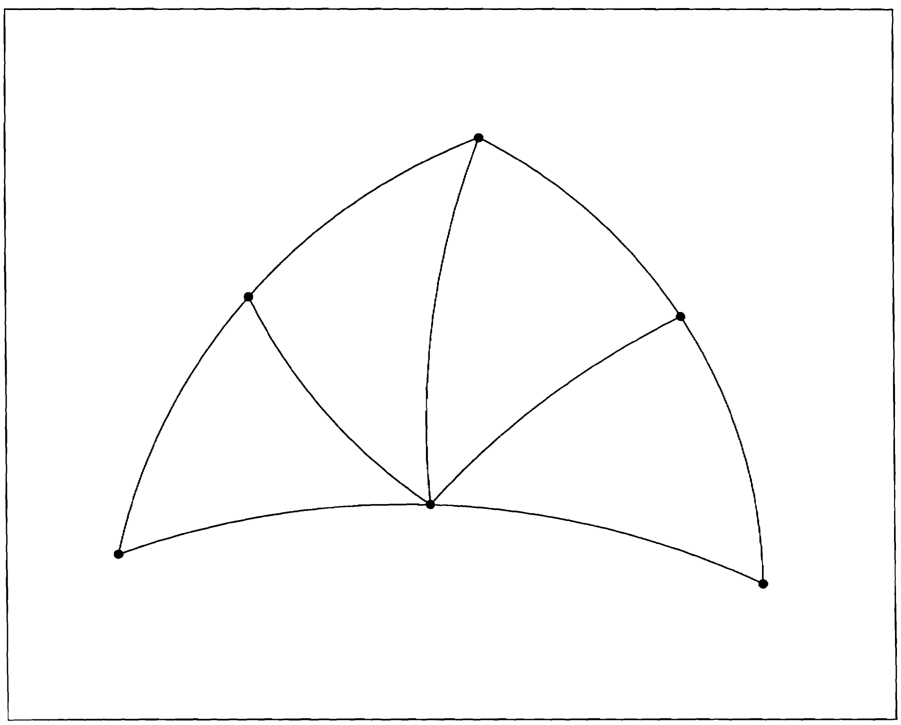

Figure 6: Spherical binary subdivision.